

# Journal of Visualized Experiments

## A robust method for the large-scale production of spheroids for high-content screening and analysis applications --Manuscript Draft--

Article Type:	Invited Methods Collection - JoVE Produced Video
Manuscript Number:	JoVE63436R1
Full Title:	A robust method for the large-scale production of spheroids for high-content screening and analysis applications
Corresponding Author:	Jeremy C. Simpson University College Dublin Dublin, IRELAND
Corresponding Author's Institution:	University College Dublin
Corresponding Author E-Mail:	jeremy.simpson@ucd.ie
Order of Authors:	Alannah S. Chalkley Margaritha M. Mysior Jeremy C. Simpson
Additional Information:	
Question	Response
Please specify the section of the submitted manuscript.	Biology
Please indicate whether this article will be Standard Access or Open Access.	Standard Access (\$1400)
Please indicate the <b>city, state/province, and country</b> where this article will be <b>filmed</b> . Please do not use abbreviations.	Dublin, Ireland
Please confirm that you have read and agree to the terms and conditions of the author license agreement that applies below:	I agree to the <a href="#">Author License Agreement</a>
Please confirm that you have read and agree to the terms and conditions of the video release that applies below:	I agree to the <a href="#">Video Release</a>
Please provide any comments to the journal here.	

**TITLE:**

A Robust Method for the Large-Scale Production of Spheroids for High-Content Screening and Analysis Applications

**AUTHORS AND AFFILIATIONS:**

Alannah S. Chalkley, Margaritha M. Mysior, Jeremy C. Simpson\*

Cell Screening Laboratory, UCD School of Biology and Environmental Science, University College Dublin, Dublin, Ireland.

Email addresses of co-authors:

Alannah S. Chalkley (alannah.chalkley@ucdconnect.ie)

Margaritha M. Mysior (margaritha.mysior@ucd.ie)

Jeremy C. Simpson (jeremy.simpson@ucd.ie)

\*Corresponding author

Jeremy C. Simpson (jeremy.simpson@ucd.ie)

**SUMMARY:**

This protocol details a method for the production of three different types of spheroids in a manner that makes them suitable for large-scale high-content screening and analysis. In addition, examples are presented showing how they can be analyzed at spheroid and individual cell levels.

**ABSTRACT:**

High-content screening (HCS) and high-content analysis (HCA) are technologies that provide researchers with the ability to extract large-scale quantitative phenotypic measurements from cells. This approach has proved powerful for deepening our understanding of a wide range of both fundamental and applied events in cell biology. To date, the majority of applications for this technology have relied on the use of cells grown in monolayers, although it is increasingly realized that such models do not recapitulate many of the interactions and processes that occur in tissues. As such, there has been an emergence in the development and use of 3-dimensional (3D) cell assemblies, such as spheroids and organoids. Although these 3D models are particularly powerful in the context of cancer biology and drug delivery studies, their production and analysis in a reproducible manner suitable for HCS and HCA present a number of challenges. The protocol detailed here describes a method for the generation of multicellular tumor spheroids (MCTS), and demonstrates that it can be applied to three different cell lines in a manner that is compatible with HCS and HCA. The method facilitates the production of several hundred spheroids per well, providing the specific advantage that when used in a screening regime, data can be obtained from several hundred structures per well, all treated in an identical manner. Examples are also provided, which detail how to process the spheroids for high-resolution fluorescence imaging and how HCA can extract quantitative features at both the spheroid level as well as from individual cells within each spheroid. This protocol could easily be applied to answer a wide range of important questions in cell biology.

## INTRODUCTION:

Traditionally, cell-based assays have been performed in monolayers growing on a solid substrate, which effectively can be considered as a two-dimensional (2D) environment. However, it is becoming increasingly recognized that 2D cell culture models lack physiological relevance in some contexts and cannot replicate many of the complex interactions that occur between cells<sup>1</sup>. Three-dimensional (3D) cell culture methods are rapidly becoming popular among researchers, and 3D cell models show high potential to better mimic the physiological conditions encountered by cells in the tissue environment<sup>2</sup>. There are several different types of 3D cell assemblies that have been employed, but the two most common types are spheroids and organoids. Spheroids can be grown from many different cell lines, and they can adopt various shapes and sizes depending on the cell type used and their method of assembly<sup>3</sup>. Moreover, spheroids can also be referred to as multicellular tumor spheroids (MCTS) when they are grown from cancer cell lines, and these models have found particular use for preclinical *in vitro* drug delivery and toxicity studies<sup>4,5</sup>. Organoids, on the other hand, aim to better mimic the tissues and organs in our body and can adopt more complex morphological arrangements. The production of organoids involves the use of adult stem cells or pluripotent stem cells, which can be reprogrammed into the appropriate cells to resemble the tissue or organ of interest. They are primarily used to investigate the development of organs and to model diseases and host-pathogen interactions<sup>6</sup>.

There is a range of different methods used to generate 3D cell assemblies. Scaffold-based methods provide a substrate or support to which cells can either attach or grow within. These scaffolds can have various shapes and can be made from a variety of different materials. The most common are extracellular matrix (ECM) components and hydrogels, and they are designed to resemble the natural extracellular environment of cells and thereby facilitate physiological interactions<sup>4,7</sup>. ECM basement material has been extracted from Engelbreth-Holm-Swarm mouse sarcoma tumor and shown to contain a rich mixture of ECM components, including laminin, type IV collagen, and perlecan<sup>8</sup>. However, despite its advantageous composition, there are two main challenges with its use, namely its batch-to-batch variability and that it has two different aggregate states below and above 10 °C<sup>8,9</sup>. In contrast, hydrogels have the advantage of being flexible with respect to their components and rigidity, and they can be customized to suit the specific 3D cell assembly desired<sup>7,10</sup>. Scaffold-based methods are essential for organoid growth but are also widely used for spheroids. Scaffold-free methods, which work by preventing cells from attaching to the surface they are growing on, are usually only compatible with spheroid assembly. Examples include ultra-low attachment (ULA) plates, with either a flat bottom or U-bottom, which allow aggregation of the cells into spheroids, or the use of continuous agitation of the cells in spinner/rotation flasks<sup>10</sup>.

The use of 3D cell assemblies to study a wide variety of biological events is rapidly gaining popularity; however, it is essential that the method chosen for their culture is appropriate and compatible with the plans for their downstream analysis. For example, the use of ULA plates generates spheroids of high consistency; however, this method is restricted to the production of a single spheroid per well, thereby limiting throughput. Particular consideration is needed when fluorescence imaging of the 3D structure is planned. The substrate or plate on which the assembly is grown needs to be optically compatible, and care must be taken to minimize the

effects of light scattering caused by any scaffolds that may have been used<sup>11</sup>. This particular problem becomes more acute as the numerical aperture of the microscope objective lenses increases.

Arguably one of the major reasons for selecting to work with a 3D cell model is to extract volumetric imaging data about not only the entire assembly but also the individual cells within it. MCTS models, in particular, are beginning to prove very powerful for deepening our understanding of how therapeutics transit from the outside to central cells (as they would need to in a tumor)<sup>12</sup>, and so gaining knowledge from individual cells at different layers is essential. The imaging technology that extracts quantitative information from individual cells is termed high-content analysis (HCA) and is a powerful approach in the context of screening<sup>13</sup>. To date, HCA has almost exclusively been applied to monolayer cultures, but there is an increasing realization that this approach has the power to be applied to 3D cultures enabling a wide range of cellular functions and processes to be studied<sup>14</sup>. It would have the clear advantage that large numbers of 3D assemblies could be analyzed, potentially providing cell-level data from across each structure. However, challenges associated with imaging of potentially thick cell assemblies, as well as the large data sets generated, need to be overcome.

In this article, a robust scaffold-based method for the large-scale production of MCTS in a 96-well format is presented. The method facilitates the production of several hundred 3D cell assemblies in each well. Examples are shown for three different cell types, representing solid tumor models of the liver, lung, and colon. The spheroids that form can be of a variety of sizes, and so HCA is used to select structures of a particular size and/or morphology. This feature provides the additional advantage that any phenotypes observed can be compared across spheroids of different sizes, but all treated in the same way in the same well. This approach is compatible with high-resolution imaging, importantly providing both cell-level and subcellular level quantitative data from the same cellular assemblies. This method of spheroid production has the additional advantage over methods that generate a single spheroid per well, that the large numbers of spheroids produced in each well potentially provide sufficient biomass for other downstream analyses, such as transcriptome and proteome profiling.

## **PROTOCOL:**

### **1. Cell culture**

#### **1.1. Prepare media**

1.1.1. Prepare specific cell culture media depending on the type of cell line. Ensure that all media for cell maintenance contains 10% Foetal Bovine Serum (FBS).

NOTE: Different cell lines use different media. HT-29 colon carcinoma cells (ATCC HTB-38) are grown in McCoy's 5A + 10% FBS. HepG2 hepatocellular carcinoma cells (ATCC HB-8065) are grown in Minimum Essential Medium + 1% L-glutamine + 10% FBS. H358 bronchoalveolar carcinoma cells (ATCC CRL-5807) are grown in RPMI 1640 medium + 1% L-glutamine + 10% FBS. All media

containing L-glutamine and FBS are referred to as complete media. When plating cells to grow as spheroids, a phenol red-free medium with 10% FBS is required to avoid coloring of the ECM basement material, which in turn can cause artifacts during the imaging process.

## 1.2. Subculture cells

1.2.1. When cells are approximately 80% confluent, wash briefly with 2 mL of trypsin-EDTA (0.25% (w/v) trypsin/0.53 mM EDTA). Aspirate the trypsin-EDTA, add 3 mL of fresh trypsin-EDTA and incubate for 3–5 min at 37 °C.

1.2.2. When cells are detached from the cell culture dish, add 7 mL of fresh complete medium.

1.2.3. Pipette 1 mL of cell suspension into a new 10 cm cell culture dish and add 9 mL of fresh complete medium to give a 1:10 dilution of cells.

1.2.4. Culture the cells at 37 °C in a humidified incubator with 5% CO<sub>2</sub>.

1.2.5. Subculture the cells every 3–5 days, depending on the cell line.

## 2. Generation of spheroids

### 2.1. Coat 96-well plates with ECM basement material

2.1.1. Thaw ECM basement material on ice overnight.

2.1.2. Dilute ECM basement material in cold phenol red-free serum-free medium using pre-chilled tips kept at -20 °C.

NOTE: The final concentration of ECM basement material depends on the cell line used. For HT-29 and H358 cells, use 4 mg·mL<sup>-1</sup> of ECM basement material. For HepG2 cells, use 4 mg·mL<sup>-1</sup> of reduced growth factor ECM basement material.

2.1.3. Pipette 15 µL of the ECM basement material/medium solution into a 96-well imaging plate.

NOTE: For large-scale spheroid production, this step can be performed with both an 8-channel pipette and a 96-channel pipetting head, as long as the tips and reservoir containing the ECM basement material are chilled.

2.1.4. Centrifuge the plate for 20 min at 91 x g at 4 °C.

2.1.5. Incubate the plate for no longer than 30 min at 37 °C.

### 2.2. Subculture and count cells

2.2.1. During the plate incubation period, incubate the cells with trypsin-EDTA and resuspend them in a complete medium containing 10% FBS.

2.2.2. Pipette 10  $\mu\text{L}$  of the cell suspension into a hemocytometer counting chamber. Count the number of cells in 4 quadrants of the chamber.

2.2.3. Calculate the number of cells within the cell suspension by determining the mean number of cells within the 4 quadrants.

NOTE: Cells can also be counted using automated cell-counting devices.

2.2.4. Centrifuge the cells at  $135 \times g$  for 4 min at room temperature (RT).

2.2.5. Once the cells are pelleted, aspirate the supernatant and resuspend the cells in a phenol red-free complete medium to obtain a concentration of  $1 \times 10^6$  cells per mL.

2.3. Seed cells into ECM basement material-coated plates

2.3.1. Dilute the cells in a phenol red-free complete medium.

NOTE: The density of cells seeded is dependent on the cell line used. For HT-29 and HepG2 cells,  $3 \times 10^4$  cells are seeded per well; for H358 cells,  $4 \times 10^4$  cells are seeded per well.

2.3.2. Seed the cells in a total volume of 35  $\mu\text{L}$  per well. Ensure to add them dropwise in a circular motion.

NOTE: For large-scale spheroid production, this step can be performed with an 8-channel pipette, as long as the pipetting circular motion can be achieved.

2.3.3. Incubate the cells for 1 h at  $37^\circ\text{C}$  in a humidified incubator with 5%  $\text{CO}_2$ .

2.3.4. Prepare a solution of ECM basement material in phenol red-free complete medium, which results in a final concentration of 2% ECM basement material in the well. To achieve this, add 1.2  $\mu\text{L}$  of ECM basement material to 23.8  $\mu\text{L}$  of phenol red-free complete medium per well, resulting in a final volume of 60  $\mu\text{L}$  per well.

2.3.5. Incubate the cells at  $37^\circ\text{C}$  in a humidified incubator with 5%  $\text{CO}_2$ .

2.3.6. The following day, replace the medium with 100  $\mu\text{L}$  of fresh phenol red-free complete medium.

2.3.7. Replace the medium every second day with 100  $\mu\text{L}$  of fresh phenol red-free complete medium.

### 3. Immunofluorescence staining of spheroids

NOTE: This protocol is adapted from Nürnberg et al., 2020<sup>15</sup>. These adaptations are primarily based on the fact that the spheroids described in this protocol are smaller than those used in the Nürnberg et al. work<sup>15</sup> and, as such, facilitate shorter incubation times. For example, blocking times are reduced from 2 h to 1 h. In addition, as the protocol is designed for high-throughput production of spheroids, all of the processing steps are carried out in the well in which the spheroids are cultured, meaning that transfer of individual spheroids into tubes is not required.

3.1. Prepare all solutions and buffers required for fixing and staining

3.1.1. Prepare Phosphate Buffered Saline (PBS) by adding 1 PBS tablet per 200 mL of water. Autoclave the PBS.

3.1.2. Prepare paraformaldehyde (PFA) following steps 3.1.3–3.1.4.

3.1.3. Use a heated stirrer to heat 400 mL of PBS to 60–70 °C in a fume hood. Add 15 g of PFA while stirring. Once the PFA has dissolved, add 50 µL of 1 M CaCl<sub>2</sub> and 50 µL of 1 M MgCl<sub>2</sub>.

3.1.4. Add 100 mL of PBS to make a final volume of 500 mL. Use NaOH to equilibrate the PFA to pH 7.4. Filter the PFA through sterile vacuum filters (pore size 0.22 µm), aliquot, and store at -20 °C.

3.1.5. Prepare a 1 M glycine stock solution by adding 3.75 g of glycine to 50 mL of PBS. Store at 4 °C.

3.1.6. Prepare 5 mL of permeabilization buffer by adding 100 µL of Triton X-100, 1 mL of dimethyl sulfoxide (DMSO) and 1.5 mL of 1 M glycine to 2.4 mL of PBS. Store at 4 °C for no longer than 2 weeks.

3.1.7. Prepare 5 mL of blocking buffer by adding 100 µL of Triton X-100, 0.5 mL of DMSO and 0.05 g of bovine serum albumin (BSA) to 4.9 mL of PBS. Aliquot the blocking buffer into 1.5 mL tubes and store at -20 °C.

3.1.8. Prepare 5 mL of antibody incubation buffer by adding 10 µL of polysorbate 20, 0.05 g of BSA, and 250 µL of DMSO to 4.74 mL of PBS. Aliquot the antibody incubation buffer into 1.5 mL tubes and store it at -20 °C.

NOTE: In the protocol described here, spheroids are only assembled in the inner 60 wells of a 96-well plate, although they can be prepared in all 96 wells of the plate. The reason for only preparing spheroids in the inner 60 wells is that some high numerical aperture objective lenses are not capable of physically being able to image the entire well of the outer wells due to the

‘skirt’ on some plate types. The above volumes are sufficient for the preparation of 60 wells containing spheroids.

### 3.2. Fix and permeabilize the spheroids

3.2.1. Carefully remove the medium from the spheroids, ensuring that the ECM basement material layer is not disturbed.

3.2.2. Wash the spheroids twice with 70  $\mu$ L of PBS for 3 min each time.

3.2.3. Fix the spheroids with 70  $\mu$ L of 3% PFA for 1 h at 37 °C.

3.2.4. Wash the spheroids twice with 70  $\mu$ L of PBS for 3 min each time.

3.2.5. Quench with 70  $\mu$ L of 0.5 M glycine solution for 30 min at 37 °C.

3.2.6. Permeabilize the spheroids using 70  $\mu$ L of the permeabilization buffer for 30 min at RT.

3.2.7. Wash the spheroids twice with 70  $\mu$ L of PBS for 3 min each time.

3.2.8. Incubate the spheroids in 70  $\mu$ L of blocking buffer for 1 h at 37 °C.

NOTE: Once the spheroids have been fixed, all subsequent processing steps can be performed using an 8-channel pipette, or a 96-well pipetting head, if available. This increases the speed of spheroid preparation prior to imaging.

### 3.3. Immunostain spheroids using primary and secondary antibodies

3.3.1. Dilute the primary antibody to an appropriate dilution in the antibody incubation buffer and add 70  $\mu$ L to each well. Incubate the spheroids with the primary antibody overnight.

NOTE: The dilution depends on the specific antibody used. In the example shown here, lysosomes are immunostained with mouse anti-LAMP1 antibodies using a dilution of 1:500.

3.3.2. The following day, wash the spheroids 5 times with 70  $\mu$ L of PBS for 3 min each time.

3.3.3. Dilute the secondary antibody at a dilution of 1:500, fluorescently-conjugated phalloidin at 1:500, and Hoechst 33342 (from a 1 mg mL<sup>-1</sup> stock) at 1:5000 in the antibody incubation buffer and add 70  $\mu$ L to each well. Incubate overnight.

NOTE: The antibody dilution depends on the specific antibody used. Highly cross-adsorbed secondary antibodies that show high photostability and high brightness are recommended.

3.3.4. The following day, wash the spheroids 5 times with 70  $\mu$ L of PBS for 3 min each time.



NOTE: Plates can be stored for up to two weeks at RT prior to imaging, as long as the spheroids remain covered with PBS.

#### 4. Image acquisition and analysis of spheroids

##### 4.1. Image acquisition

4.4.1. Insert the 96-well plate containing spheroids into a confocal high-content screening microscope.

4.4.2. Select the appropriate lasers to excite the fluorophores used.

4.4.3. Acquire the channels sequentially to avoid cross-talk.

4.4.4. Image the spheroids using appropriate objectives.

NOTE: The use of water immersion objectives is recommended if available. For example, a 20x/1.0 NA objective can image an entire well in ~77 fields of view. A 63x/1.15 NA objective can image an entire well in approximately 826 fields of view.

4.4.5. Image ~30–40 slices, depending on the depth of the spheroid, with each slice taken at an interval of 1.5  $\mu\text{m}$  from the preceding one.

##### 4.2. Image analysis

4.2.1. For morphological analysis of spheroids, follow steps 4.2.2–4.2.6.

4.2.2. Segment the spheroids based on the fluorescently-conjugated phalloidin staining.

4.2.3. Segment the nuclei based on the Hoechst 33342 staining.

4.2.4. Segment the cytoplasm of each cell by the residual Hoechst 33342 stain that is present in the cell cytoplasm.

4.2.5. Calculate different morphological properties of the spheroids, including volume, surface area, sphericity, and the number of nuclei per spheroid.

NOTE: This information is extracted using various algorithms that are in-built in the image analysis software of choice.

4.2.6. Process images further to remove spheroids smaller than 75,000  $\mu\text{m}^3$  and larger than 900,000  $\mu\text{m}^3$ .

NOTE: These values are suggestions to allow the removal of very small cell assemblies and large assemblies that may have arisen as a result of the fusion of multiple spheroids. Spheroids can also be categorized into different size classes at this step.

4.2.7. To analyze single cells within spheroids, follow steps 4.2.8–4.2.12.

4.2.8. Segment the spheroids based on the fluorescently-conjugated phalloidin staining.

4.2.9. Segment the nuclei based on the Hoechst 33342 staining.

4.2.10. Segment the cytoplasm of each cell by the residual Hoechst 33342 stain that is present in the cell cytoplasm.

4.2.11. Segment the lysosomes based on the secondary antibody staining.

4.2.12. Calculate different morphological properties of the cells within each spheroid, including the number of lysosomes per cell, cell volume, and cell surface area.

NOTE: This information is extracted using various algorithms that are in-built in the image analysis software of choice.

#### REPRESENTATIVE RESULTS:

In this protocol, a robust method to produce 3D cell culture assemblies in the form of spheroids, using different cell types to represent various tumor tissues, is detailed. This method allows for the generation of hundreds of spheroids per well, which enables cell-based assays to be performed in a high-content manner (**Figure 1**). This approach has previously been used to study nanoparticle uptake in HT-29 spheroids<sup>16</sup> and nanoparticle-induced toxicity in HepG2 spheroids<sup>17</sup>. The method relies on producing a thin and even distribution of scaffold material across the well bottom of an optical quality plate. Cells are seeded into each well, and further scaffold material, at a low concentration, is added as an overlay on the cells. This results in a base that supports even growth of spheroids, meaning that several hundred spheroids can be cultured in each well of a 96-well plate. A low magnification objective is used to generate an overview image of the entire population (**Figure 2**). Sub-regions of the well can then be selected and imaged using a high-resolution objective, and in each position, a complete confocal stack is acquired. This provides the necessary information for subsequent volumetric analysis of each spheroid.

The individual spheroids can then be analyzed by HCA, thereby providing information about the morphological properties of the spheroids. Typically the first step is to identify each spheroid as a single object. To do this, a fluorescence channel that is likely to give consistent staining or distribution throughout the spheroid is selected. In the example shown here, the signal in the fluorescently-conjugated phalloidin channel is used, as actin is found close to the plasma membrane in all cells in the different spheroid types (**Figure 2** and **Figure 3A**). As a result of complete confocal stacks being generated, all HCA steps can be carried out in a volumetric

manner rather than on a slice by slice basis. This is important as it removes any bias associated with the analysis of a small number of selected planes. This volumetric approach is then applied to the other channels in the image. The nuclei were detected and segmented based on the Hoechst 33342 staining, and this same channel can be used to detect the cell cytoplasm, as there is residual Hoechst 33342 present at low levels (**Figure 3B**). If downstream analysis of individual cells within the spheroid is needed, the other channels (for example, lysosomes immunostained with anti-LAMP1 antibodies) can also be processed in a similar manner. The volumetric approach allows all fluorescently-labeled structures to be visualized from all views (**Figure 3C**).

Having identified the spheroid as a distinct object, various morphological measurements at the spheroid level can be made. These measurements include calculation of the number of nuclei per spheroid (**Figure 4A**), as well as the sphericity (**Figure 4B**), volume (**Figure 4C**), and surface area (**Figure 4D**) of the spheroid. Depending on the HCA software used, other morphological features such as cross-sectional area, inner disk radius, and inner sphere radius can also be calculated. In the examples shown here, spheroids below 75,000  $\mu\text{m}^3$  and above 900,000  $\mu\text{m}^3$  were discarded from the measurements, but these parameters can be set by the user, depending on the desired spheroid properties for analysis. Spreadsheets were generated by the image analysis software and imported into RStudio for analysis. Boxplot graphs were produced to display the morphological properties of the different types of spheroids (**Figure 4**). These boxplots reveal the level of spheroid heterogeneity in the population, which is why it is important to quantify a large number of spheroids in any one experiment. This is a key advantage over methods that generate a single spheroid per well. The three spheroid types shown here show a high level of similarity with respect to their volume and surface area, although it is notable that the sphericity of HepG2 spheroids is somewhat lower than that of the other types shown here (**Figure 4B**).

Imaging spheroids with a high-resolution objective, such as the 63x water immersion objective used here, allows subcellular resolution of individual cells within the spheroid to be achieved. The different organelles can be segmented depending on the antibodies used. In the example shown here, lysosomes were identified based on immunostaining using anti-LAMP1 antibodies, followed by secondary antibody addition (**Figure 3C**). The segmentation of each organelle within each cell then allows the quantification of cell-level measurements. The typical volume of each cell in the three spheroid types (**Figure 5A**), as well as the number of lysosomes per cell (**Figure 5B**), are shown. The need for such subcellular detail is determined by the assay in which the spheroids will be used.

Optimizing the initial cell seeding density at the start of spheroid generation is a critical step. Adding too many cells still allows spheroid formation; however, this can result in the fusion of spheroids (**Figure 6**). This leads to the generation of irregularly shaped assemblies, which in turn can be highly problematic for the downstream identification of the spheroids. When spheroids are incorrectly identified as distinct structures, there can also be problems with the analysis of the individual cells. As such, careful optimization of each cell line used for the spheroid generation, including the cell seeding density and length of growth time, are critical parameters to establish.

## FIGURE AND TABLE LEGENDS:

**Figure 1: Schematic detailing the protocol used to generate spheroids for HCS and HCA.** 96-well plates are coated with a layer of ECM basement material, followed by seeding of cells, which then initiate spheroid formation. Medium is replaced the following day and every second day thereafter. In preparation for imaging, spheroids are fixed, permeabilized, and immunostained with specific antibodies. Spheroids are then imaged using a confocal HCS microscope. Graphic created with BioRender.com.

**Figure 2: Example images of H358, HepG2, and HT-29 spheroids.** Fully automated HCS confocal imaging of (A) H358, (B) HepG2, and (C) HT-29 spheroids. Panels show a single well overview, as well as three example confocal slices and the volumetric reconstruction of one spheroid from each cell line. Nuclei stained with Hoechst 33342 are shown in blue, actin stained with fluorescently-conjugated phalloidin in red, and lysosomes immunostained for LAMP1 in green. Images of the well overview were acquired with a 20x water immersion objective (NA 1.0). Images of individual spheroids were acquired with a 63x water immersion objective (NA 1.15).

**Figure 3: Example key steps in image analysis.** (A) Each spheroid is first identified in volumetric mode by detection of the fluorescently-conjugated phalloidin staining. (B) Using this information as a mask, the cytoplasm of each cell is segmented by the residual Hoechst 33342 stain that is present in the cell cytoplasm. The nuclei are segmented by the Hoechst 33342 stain. The lysosomes are segmented using the antibody (anti-LAMP1) immunostaining. Volumetric views are shown. (C) 3-plane views of the same spheroid. The example shown is of a H358 cell spheroid. Images were acquired with a 63x water immersion objective (NA 1.15)

**Figure 4: Examples of spheroid-level measurements.** All measurements were made using an automated image analysis pipeline, and for three types of spheroids, namely H358, HepG2 and HT-29, imaged with a 20x objective. Shown are (A) mean number of nuclei per spheroid, (B) spheroid sphericity, (C) spheroid volume, and (D) spheroid surface area. All boxplots show the median value and quartiles for each spheroid type. Data are from 3 replicate wells; the total number of spheroids analyzed were 1259 (H358), 1522 (HepG2), and 1326 (HT-29). Images were acquired with a 20x water immersion objective (NA 1.0).

**Figure 5: Examples of cell-level measurements from spheroids.** All measurements were made using an automated image analysis pipeline, and for three types of spheroids, namely H358, HepG2, and HT-29, imaged with a 63x objective. Shown are (A) volumes of individual cells, and (B) mean numbers of lysosomes per cell. The total number of cells analyzed were 1410 (H358), 1625 (HepG2), and 1401 (HT-29), from 20 spheroids of each cell line. Images were acquired with a 63x water immersion objective (NA 1.15)

**Figure 6: Example images showing effects of over-plating of cells on spheroid formation.** Example images are shown for H358, HepG2, and HT-29 spheroids. Arrows indicate places where spheroids have likely fused. Images were acquired with a 20x water immersion objective (NA 1.0).

## DISCUSSION:

The approach described here details a platform for generating several hundred spheroids per well in a manner that is suitable for HCS and HCA. In comparison to other popular methods, such as the use of flat-bottomed and round-bottomed ULA plates, which allow the formation of only one spheroid per well<sup>18,19</sup>, this method provides the opportunity for high-resolution information to be extracted from large numbers of spheroids in a screening format. Notably, this method has been demonstrated in 3 different cell lines, representing various tumor types, highlighting its broad suitability to study a range of cellular processes in different models. Although the spheroids generated using this method shows some variability in size and shape, HCA can easily classify them by size (or any other parameters of interest). Our lab has successfully used this approach to study nanoparticle-induced toxicity as a function of spheroid size. Importantly, all the different size classes of spheroids can be studied in the same well, meaning that all were exposed to identical treatments, giving highly robust outputs from a large spheroid population<sup>17</sup>. The methodology described here could easily be adapted for use with other cell types representing different tissues. In addition, such spheroids could be used to assess different biological processes<sup>14</sup>. If the spheroids are generated with cells stably expressing fluorescently-tagged proteins, live cell imaging is also possible.

One critical step in this protocol is the production of the ECM basement material layer on which the cells are plated. When the layer is too thick, it can form a meniscus<sup>20</sup> that promotes the growth of monolayers in the center of the well and spheroids only at the outer rims of the well. Therefore, it is essential that the correct concentration and volume of the ECM basement material is chosen to allow uniform spheroid formation throughout the well; this is always cell line-dependent. Also of note is that excess ECM basement material can cause issues during the immunostaining process, as it is not easily dissolved. This can in turn, lead to complications during image acquisition when using a HCS confocal microscope system. One other consideration is that different cell lines can require different ECM formulations. For example, HepG2 spheroids require ECM basement material with a reduced concentration of growth factors, compared to that used by H358 and HT-29 spheroids. The method of cell plating is also important, as this determines how the cells are distributed in the well. When either too many cells are seeded or when they are poorly distributed, this can lead to spheroid fusion (**Figure 6**). One other challenge of using ECM scaffolds is that they need to be handled at low temperatures (below 10 °C), which is particularly problematic when using automation for HCS. However, this problem was recently solved by Eismann and colleagues (2020), who employed microarray technology to spot 0.2 µL droplets of ECM basement material and cells into chambered slides. This was sufficient material to facilitate the growth of small spheroids<sup>21</sup>. Whether such an approach would also work for plating larger volumes of ECM basement material into wells of multi-well plates remains to be demonstrated.

One problem associated with the analysis of 3D cell models using microscopy is the ability to extract information from the central planes of these assemblies. In this regard, permeabilization and antibody access during the immunostaining process can be problematic. However, the protocol published by Nürnberg and colleagues<sup>15</sup> enables highly consistent immunostaining of the entire spheroid. Using slight modifications to this protocol, this technique can immunostain even small subcellular structures (for example, lysosomes), with a high degree of consistency,

regardless of whether the cells are central or peripheral with respect to the overall spheroid structure. It is important that this step is carefully optimized when using new antibodies.

Another critical step is the imaging regime chosen. Imaging the appropriate number of z-slices through the spheroid is important, as this determines the volume of data that needs to be analyzed and stored. For example, imaging a limited number of z-planes at too great an interval can result in an underestimation of the overall spheroid size and volume. On the other hand, capturing too many z-planes can result in data analysis and storage problems. Very large datasets also require more intensive computational power for their analysis, particularly in volumetric mode. The optimal sampling interval in the z-plane is largely dictated by the characteristics of the objective lens, but for the examples shown here, ca. 40 confocal slices are required at an interval of 1.5  $\mu\text{m}$  to facilitate imaging through the entire depth of the spheroid.

As mentioned, in order to reduce bias from analysis of selected planes, the use of a volumetric-based image analysis approach is strongly recommended. This allows not only spheroid-level information to be extracted but also cell-level data from each individual spheroid. Ultimately, the HCA pipelines need to be designed in such a way that they address the specific biological question being asked. Multiparametric outputs enable complex phenotypes to be quantitatively described. This has been demonstrated to work for 3D cell assemblies using commercial HCA software<sup>16,17</sup>, as well as freely-accessible software such as CellProfiler<sup>22,23</sup>. Volumetric analysis methods have the potential to be applied to other 3D cell model types, such as organoids and *ex vivo* patient-derived explants (PDEs), which even better replicate *in vivo* conditions. Recently, a high-throughput pipeline for producing brain organoids has been described<sup>24</sup>. This involves generating organoids in a 96-well plate and subsequently imaging them using a high-content screening microscope<sup>24</sup>. PDEs are highly advantageous in that they exhibit the original histology from the tumor, thus providing a cell model that recapitulates *in vivo* conditions, including features such as the tumor microenvironment<sup>25</sup>. These models can also, in principle, be immunostained, imaged, and analyzed using the approach described here<sup>26,27</sup>.

In summary, this protocol describes an accessible and robust method for the large-scale production of spheroids for HCS and HCA applications. Its applicability is shown with three different cell lines, producing spheroids that can be imaged at high resolution. This protocol also demonstrates that volumetric analysis can provide quantitative information about the spheroid population, as well as at the single-cell and subcellular levels, thereby making it useful for a wide variety of assays.

#### ACKNOWLEDGMENTS:

The authors acknowledge the support of an infrastructure research grant from Science Foundation Ireland (SFI) (16/RI/3745) to JCS. Work in the UCD Cell Screening Laboratory is supported by the UCD College of Science. ASC is funded by an Irish Research Council (IRC) Government of Ireland Postgraduate Scholarship (GOIPG/2019/68). The authors also thank all members of the lab for their input and helpful discussions. The artwork in Figure 1 was generated in BioRender.

**DISCLOSURES:**

The authors declare that there are no competing interests associated with this work.

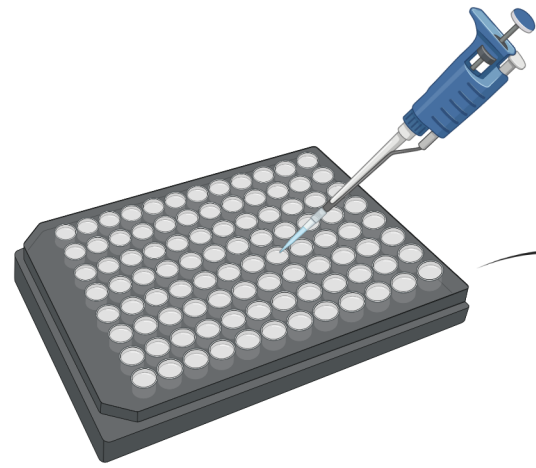
**REFERENCES:**

1. Jensen, C., Teng, Y. Is it time to start transitioning from 2D to 3D cell culture? *Frontiers in Molecular Biosciences*. **7**, 33 (2020).
2. Langhans, S. A. Three-dimensional *in vitro* cell culture models in drug discovery and drug repositioning. *Frontiers in Pharmacology*. **9**, 6 (2018).
3. Edmondson, R., Broglie, J. J., Adcock, A. F., Yang, L. Three-dimensional cell culture systems and their applications in drug discovery and cell-based biosensors. *Assay and Drug Development Technologies*. **12** (4), 207–218 (2014).
4. Lv, D., Hu, Z., Lu, L., Lu, H., Xu, X. Three-dimensional cell culture: A powerful tool in tumor research and drug discovery. *Oncology Letters*. **14** (6), 6999–7010 (2017).
5. Zhang, X., Jiang, T., Chen, D., Wang, Q., Zhang, L. W. Three-dimensional liver models: state of the art and their application for hepatotoxicity evaluation. *Critical Reviews in Toxicology*. **50** (4), 279–309 (2020).
6. Dutta, D., Heo, I., Clevers, H. Disease modeling in stem cell-derived 3D organoid systems. *Trends in Molecular Medicine*. **23** (5), 393–410 (2017).
7. Nunes, A. S., Barros, A. S., Costa, E. C., Moreira, A. F., Correia, I. J. 3D tumor spheroids as *in vitro* models to mimic *in vivo* human solid tumors resistance to therapeutic drugs. *Biotechnology and Bioengineering*. **116** (1), 206–226 (2019).
8. Kleinman, H. K., Martin, G. R. Matrigel: Basement membrane matrix with biological activity. *Seminars in Cancer Biology*. **15** (5 SPEC. ISS.), 378–386 (2005).
9. Caliri, S. R., Burdick, J. A. A practical guide to hydrogels for cell culture. *Nature Methods*. **13** (5), 405–414 (2016).
10. Foglietta, F., Canaparo, R., Muccioli, G., Terreno, E., Serpe, L. Methodological aspects and pharmacological applications of three-dimensional cancer cell cultures and organoids. *Life Sciences*. **254**, p.117784 (2020).
11. Bardsley, K., Deegan, A. J., El Haj, A., Yang, Y. Current state-of-the-art 3D tissue models and their compatibility with live-cell imaging. *Advances in Experimental Medicine and Biology*. **1035**, 3–18 (2017).
12. Darrigues, E. et al. Tracking gold nanorods' interaction with large 3D pancreatic-stromal tumor spheroids by multimodal imaging: Fluorescence, photoacoustic, and photothermal microscopies. *Scientific Reports*. **10** (1), 3362 (2020).
13. Boutros, M., Heigwer, F., Laufer, C. Microscopy-based high-content screening. *Cell*. **163** (6), 1314–1325 (2015).
14. Mysior, M. M., Simpson, J. C. Cell3: A new vision for study of the endomembrane system in mammalian cells. *Bioscience Reports*. BSR20210850 (2021).
15. Nürnberg, E. et al. Routine optical clearing of 3D-cell cultures: Simplicity forward. *Frontiers in Molecular Biosciences*. **7** (20) (2020).
16. Cutrona, M. B., Simpson, J. C. A High-throughput automated confocal microscopy platform for quantitative phenotyping of nanoparticle uptake and transport in spheroids. *Small*. **15** (37) e1902033 (2019).

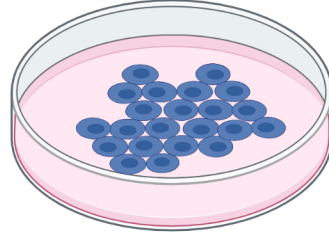
17. Kelly, S., Byrne, M. H., Quinn, S. J., Simpson, J. C. Multiparametric nanoparticle-induced toxicity readouts with single cell resolution in HepG2 multicellular tumour spheroids. *Nanoscale*. **13** (41), 17615–17628 (2021).
18. Sirenko, O., Mitlo, T., Hesley, J., Luke, S., Owens, W., Cromwell, E. F. High-content assays for characterizing the viability and morphology of 3D cancer spheroid cultures. *Assay and Drug Development Technologies*. **13** (7), 402–14 (2015).
19. Redondo-Castro, E., Cunningham, C. J., Miller, J., Cain, S. A., Allan, S. M., Pinteaux, E. Generation of human mesenchymal stem cell 3D spheroids using low-binding plates. *Bio-protocol*. **8** (16) (2018).
20. Lee, G. Y., Kenny, P. A., Lee, E. H., Bissell, M. J. Three-dimensional culture models of normal and malignant breast epithelial cells. *Nature Methods*. **4** (4), 359–365 (2007).
21. Eismann, B. et al. Automated 3D light-sheet screening with high spatiotemporal resolution reveals mitotic phenotypes. *Journal of Cell Science*. **133** (11), jcs245043 (2020).
22. Alsehli, H. et al. An integrated pipeline for high-throughput screening and profiling of spheroids using simple live image analysis of frame to frame variations. *Methods*. **190**, 33–43 (2021).
23. Stirling, D. R. et al. CellProfiler 4: improvements in speed, utility and usability. *BMC Bioinformatics*. **22** (1), 1–11 (2021).
24. Renner, H. et al. A fully automated high-throughput workflow for 3D-based chemical screening in human midbrain organoids. *eLife*. **9**, e52904 (2020).
25. Powley, I. R. et al. Patient-derived explants (PDEs) as a powerful preclinical platform for anti-cancer drug and biomarker discovery. *British Journal of Cancer*. **122** (6), 735–744 (2020).
26. Collins, A., Miles, G. J., Wood, J., MacFarlane, M., Pritchard, C., Moss, E. Patient-derived explants, xenografts and organoids: 3-dimensional patient-relevant preclinical models in endometrial cancer. *Gynecologic Oncology*, **156** (1), 251–259 (2020).
27. Miles, G. J. et al. Evaluating and comparing immunostaining and computational methods for spatial profiling of drug response in patient-derived explants. *Laboratory Investigation*. **101** (3), 396–407 (2021).



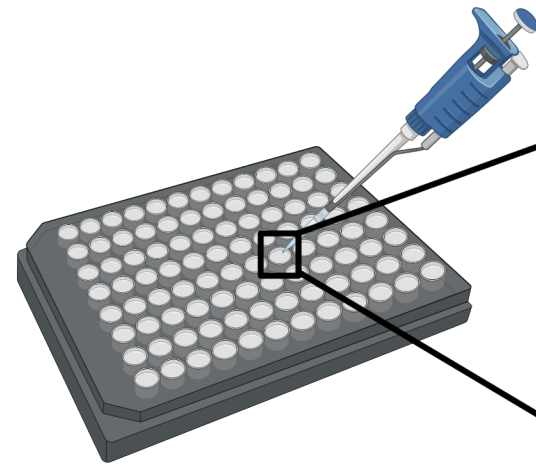
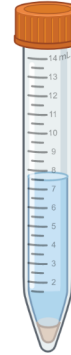
## Day 0



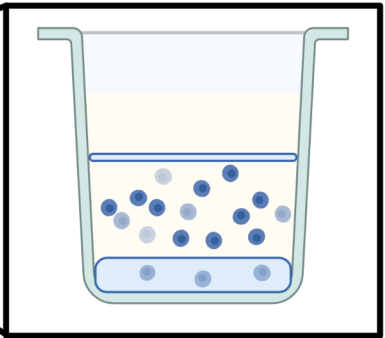
ECM basement material is diluted to the appropriate concentration and plated into a 96-well plate



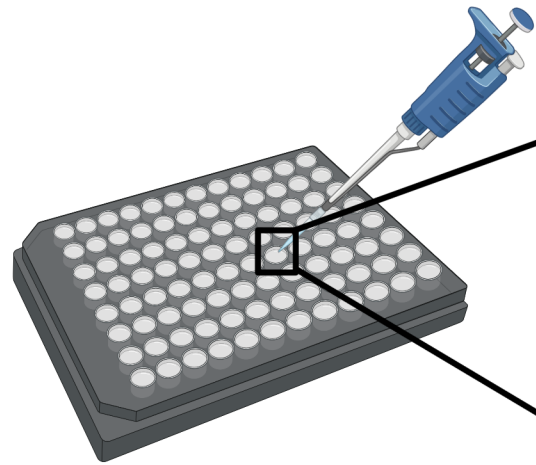
Monolayer cells are passaged and diluted in phenol red-free medium



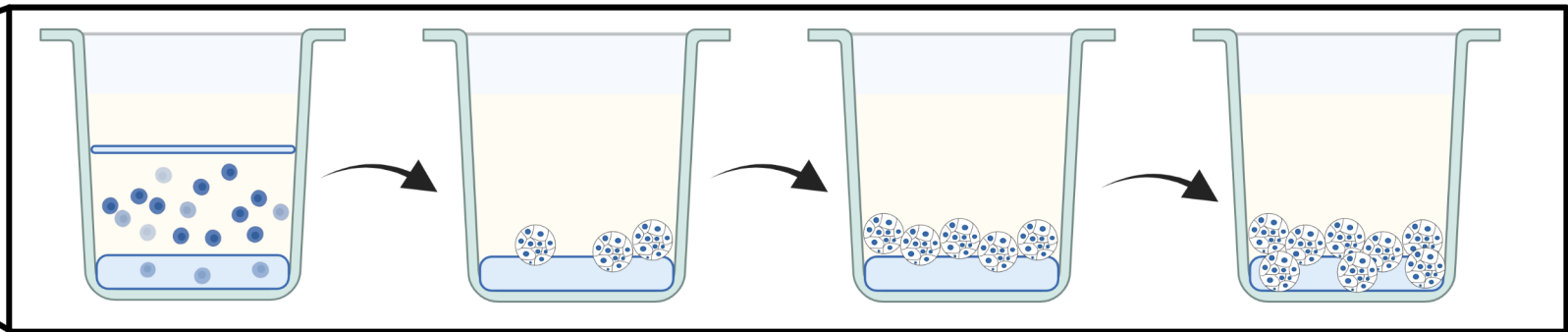
Cells are plated at the appropriate concentration into the ECM basement material-coated wells



## Day 1 - Day 7 (Cell Line Dependent)

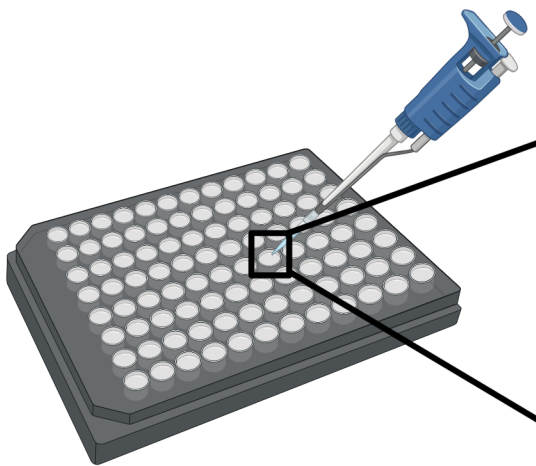


Medium is replaced the following day and every second day thereafter

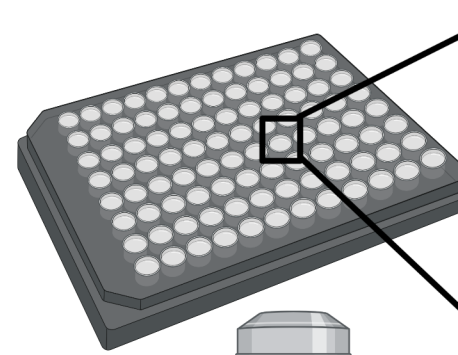
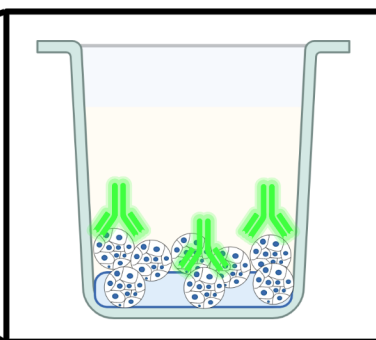


Spheroid growth is observed each day

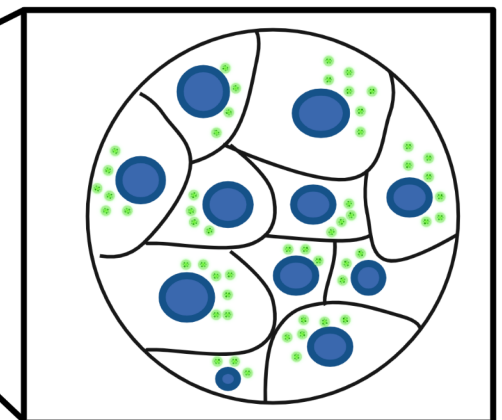
## Fixing, Processing and Imaging

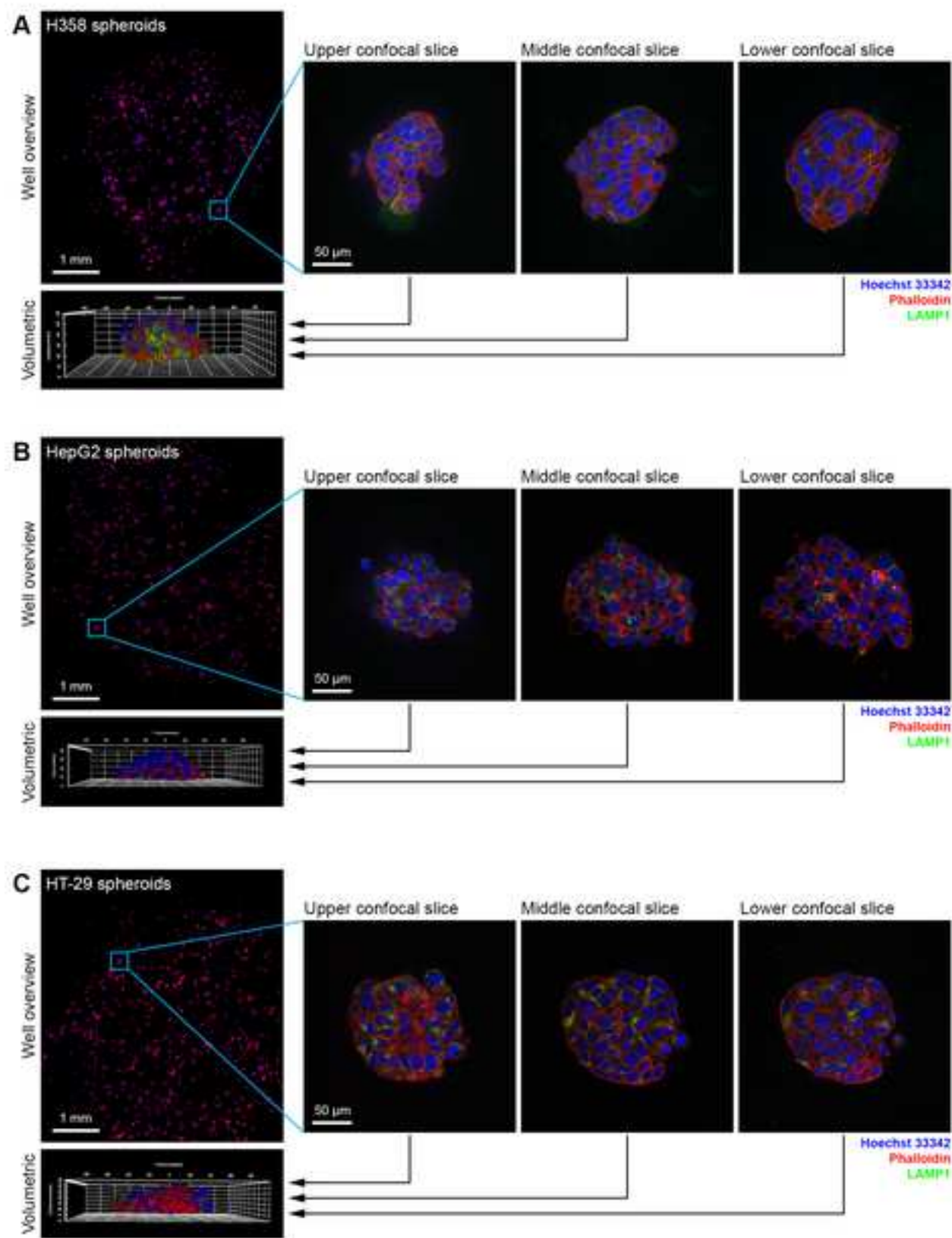


Spheroids are fixed and permeabilized, and immunostained with fluorescently-labeled antibodies against specific organelle markers



Spheroids are imaged using high-resolution objectives





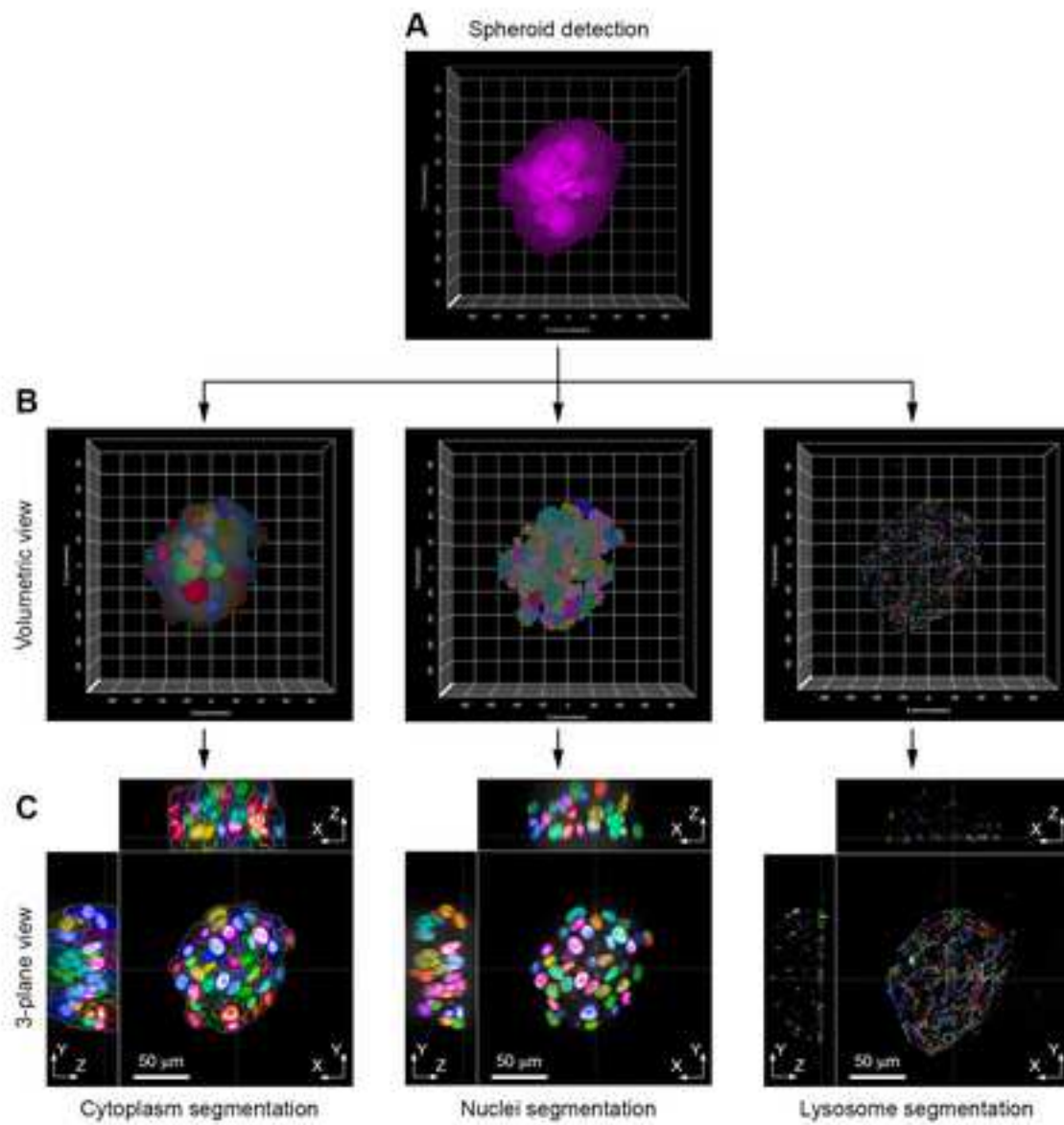
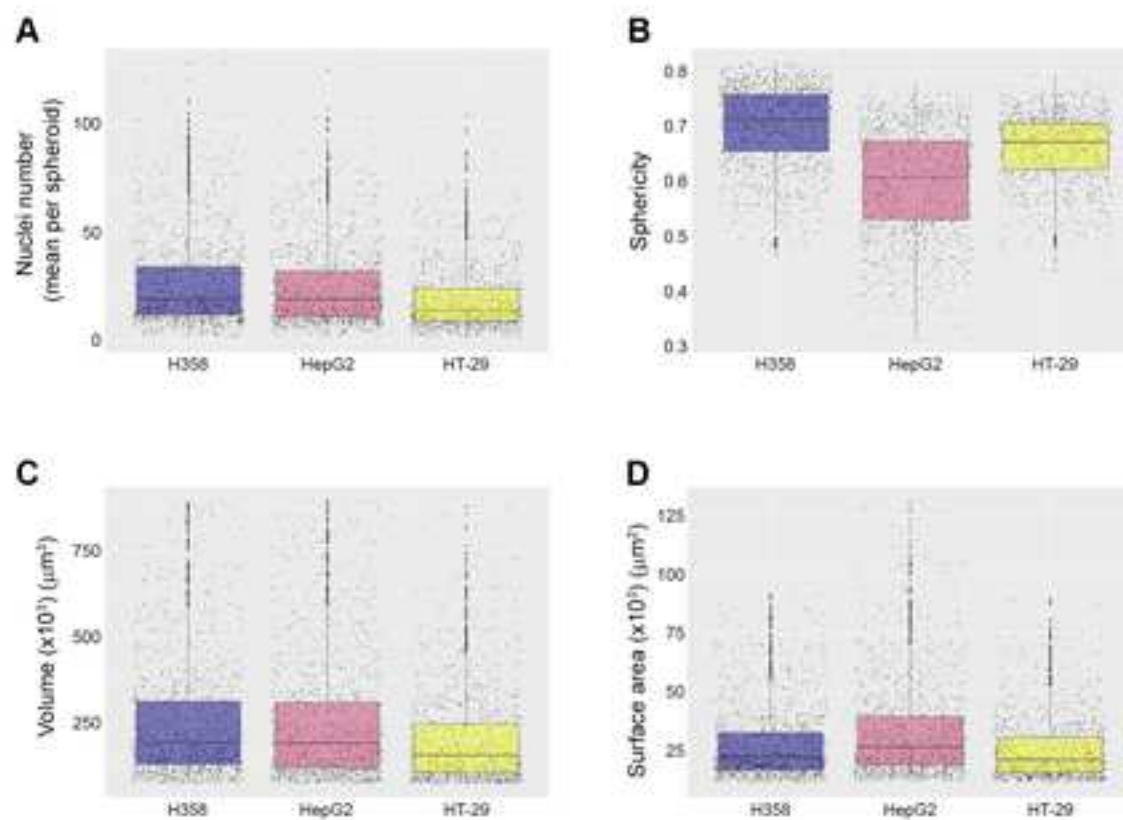
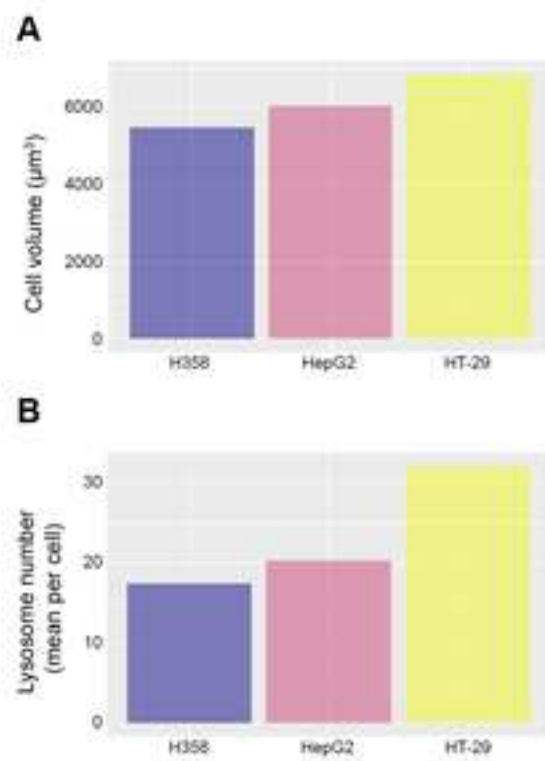
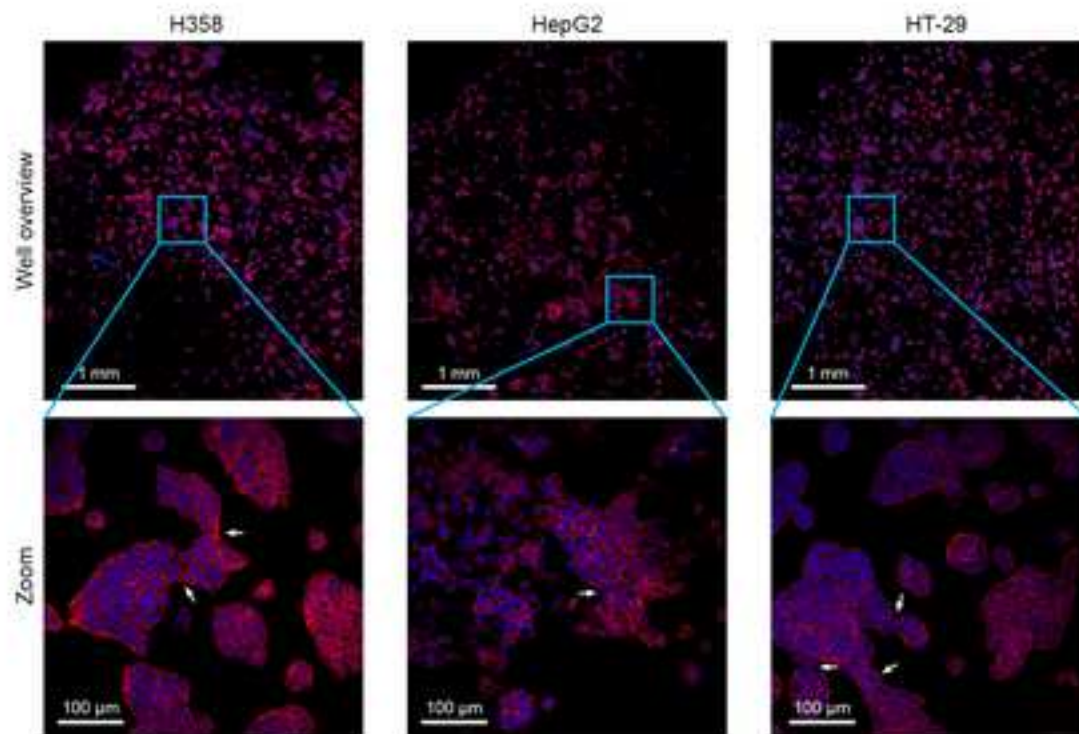



Figure 4



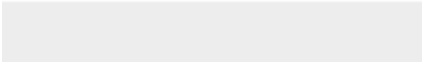









Click here to access/download  
**Table of Materials**  
Table of Materials-63436R1.xlsx



## **A robust method for the large-scale production of spheroids for high-content screening and analysis applications**

**Chalkley AS, Mysior MM & Simpson JC**

### **Response to Reviewers**

#### **Editorial comments:**

1. Please take this opportunity to thoroughly proofread the manuscript to ensure that there are no spelling or grammar issues.

**We have proofread the manuscript once more, as requested.**

2. Please provide an email address for each author.

**These have been provided in the revised manuscript.**

3. Please revise the text to avoid the use of any personal pronouns (e.g., "we", "you", "our" etc.).

**These revisions have been made to the manuscript.**

4. For in-text formatting, corresponding reference numbers should appear as numbered superscripts without brackets after the appropriate statement(s), but before the punctuation.

**These have been changed in the revised manuscript.**

5. Use h for hours and min for minutes throughout the manuscript.

**These have been changed in the revised manuscript.**

6. JoVE cannot publish manuscripts containing commercial language. This includes trademark symbols (™), registered symbols (®), and company names before an instrument or reagent. Please remove all commercial language from your manuscript and use generic terms instead. All commercial products should be sufficiently referenced in the Table of Materials (For example: Matrigel, GlutaMAX, Alexa Fluor, etc).

**These have been removed from the text of the revised manuscript.**

7. Line 48-50 and 103-106: Please provide relevant citation(s) as applicable.

**Relevant citations have been added (reference no. 2 and no. 13, respectively).**

8. Please revise the Introduction to also include the following:

- a) The advantages over alternative techniques with applicable references to previous studies
- b) A description of the context of the technique in the wider body of literature
- c) Information to help readers to determine whether the method is appropriate for their application

**We have modified the Introduction to make these points more visible. In particular, please see the new final paragraph in the Introduction section.**



9. Please adjust the numbering of the Protocol to follow the JoVE Instructions for Authors. For example, 1 should be followed by 1.1 and then 1.1.1 and 1.1.2 if necessary. Please refrain from using bullets or dashes.

We believe that the numbering guidelines have now been followed. None of the protocols use bullets or dashes.

10. Please ensure you answer the “how” question, i.e., how is the step performed? Alternatively, add references to published material specifying how to perform the protocol action. Please add more specific details (e.g., button clicks for software actions, numerical values for settings, etc.) to your protocol steps. There should be enough detail in each step to supplement the actions seen in the video so that viewers can easily replicate the protocol.

a) Line 137-138: what is the composition of complete medium? Please provide details in the Table of Materials.

Definition of complete medium is now provided in the revised manuscript.

b) Line 164: Please specify the temperature at which centrifugation was done.

This information has been added to the revised manuscript.

c) Line 223-224: Please indicate the antibody incubation buffer in the Table of Materials.

The antibody incubation buffer needs to be prepared by the user. The method for this is provided in protocol 3.1, step 6. The components of this buffer are now provided in the Table of Materials.

d) Lines 260-263, and 274-275: Please include more details of how the various geometrical properties are calculated.

These steps are specific to the software used. All high-content image analysis software allow such features to be extracted, but the precise order of buttons in the software that need to be used inevitably vary. In the examples that we show here, we have used a commercial software, and our understanding is that any specific details relating to commercial language (point 6 above) cannot be included in the protocol.

11. Step 4.2: Please ensure that all text in the protocol section is written in the imperative tense as if telling someone how to do the technique (e.g., “Do this,” “Ensure that,” etc.).

We have revised the Protocol section to ensure that it aligns with the tense required.

12. Please use a single line spacing between steps and sub steps of the protocol. Ensure that the highlight is no more than 3 pages of the Protocol (including headings and spacing) that identifies the essential steps of the protocol for the video, i.e., the steps that should be visualized to tell the most cohesive story of the Protocol.

This formatting has been added to the revised manuscript.

13. Figure 1: please correct the typo ‘appropraité’.

This typo has been corrected.

14. Figure 6: Please provide scale bars for all the panels.

These have been added to the revised figure.

15. As we are a methods journal, please ensure that the Discussion also explicitly cover the following in detail in 3-6 paragraphs with citations:

a) Any modifications and troubleshooting of the technique

We provide specific information with an associated figure on this (Figure 6).

b) Any limitations of the technique

We provide a specific example of limitations associated with the use of extracellular basement material (paragraph 2 of Discussion).

c) The significance with respect to existing methods

We provide examples of this with respect to the use of ULA plates that only generate a single spheroid per well, and that studying multiple spheroids in the same well allows a high 'n' number to be assessed in parallel (paragraph 1 of Discussion).

d) Any future applications of the technique

Examples of this are given (paragraph 1 of Discussion).

### **Reviewer #1:**

#### **Manuscript Summary:**

This manuscript describes a protocol for generating spheroids in a large-scale manner using three separate cell lines. It also provides a protocol to analyze the spheroids using high-content imaging. This manuscript is well-written and provides clear guidance. This protocol will be highly valuable to numerous researchers across multiple fields. As 3D spheroid cultures become more widely used, more standardized approaches to generation and imaging are needed. High content imaging and analysis is also in its infancy, so this approach will help many labs adapt this technology for their own studies. The graphics are helpful, clear, and aid in understanding of the protocol.

#### **Major Concerns:**

I have no major concerns.

#### **Minor Concerns:**

##### **General comments:**

- What pipettor/liquid handling is recommended or has this been tested with? Viaflo? Multi-channel? This protocol can't be high-throughput if each well is pipetted individually and it relies on very careful pipetting as to not disturb the Matrigel.

In the revised manuscript we have added further information about this. Indeed it is possible, and we routinely use 8-channel pipettes for preparation of the spheroids. The key here is to be able to plate the cells using a circular motion. Once the spheroids have been fixed, all immunostaining steps can be carried out with an 8-channel pipette, or a 96-well pipetting head.

- Can other molecular endpoints other than imaging be used with this platform? While imaging is powerful, it's helpful to have molecular endpoints as well (e.g. transcriptomics, PCR, cell viability, biomarkers). I'd recommend adding some discussion of this.

We thank the reviewer for this suggestion. We have added a comment in the Introduction that production of spheroids in this manner is also amenable for their transcriptomic and proteomic analysis.

-I recommend adding some discussion re: only being able to image halfway through a spheroid with confocal and whether adjustments are needed to volumetric calculations, etc. because of this?

In the protocol that we describe here we perform imaging through the entire spheroid, as such no adjustments are needed with respect to volumetric calculations. For the types and sizes of spheroids we culture in this manuscript, and other works that we cite (refs 16 and 17), the depth of these assemblies is below 100  $\mu\text{m}$ , which is a depth that allows easy imaging (by spinning-disc confocal microscopy) through the entire spheroid volume when the samples are prepared using this method.

Specific comments:

p.3, line 36 - Make it clearer whether it's a spheroid with three cell lines, or a spheroid with one cell line, shown with 3 different cell lines (later described as the latter but confusing in the abstract)

We agree that the wording was ambiguous. We have amended this in the revised manuscript.

p.3, line 37-38, Clarify why having several hundred spheroids per well allows this to be used in a screening regime (e.g. screening has been performed when there is one spheroid per well too). Maybe address that this provides significant/enough biomass for different cellular assays.

We agree with the reviewer that screening has been carried out in a format in which a single spheroid is grown per well. However, we would argue that this format can never be scaled up in a meaningful way, as ideally 5-10 spheroids would need to be evaluated per treatment (given potential heterogeneity between spheroids) in order to provide sufficient replicates. Given that screens might utilise hundreds or potentially thousands of compounds or RNAi reagents, the single spheroid per well approach soon becomes infeasible. One key advantage of our method is that potentially several hundred spheroids per well are generated, and all would be exposed to exactly the same treatment, given that they are growing in the same well. We do agree, however, that for other assay types where biomass is required (for example proteomic analysis), then this is an additional advantage of our approach. We have included this point in the revised manuscript.

p. 3, line 62-66 Why are PDEs described in such detail when not used for this study? Maybe describe their limitations and how this protocol may potentially be adapted to use for these systems.

We have moved the description of PDEs to the Discussion in the revised manuscript, allowing us to suggest that this may be a future application of this protocol.

p.8, line 207, Explain why only the 60 inner wells are used - add some text to the discussion or protocol re: edge effect

We have added a note about this to the protocol. The reason that we advise only using the central 60 wells, is that with some plate types, the high NA objectives are unable to image the outer wells as they physically make contact with the 'skirt' of the plate. This then precludes imaging of that entire well without potentially causing damage to the objective lens. This problem only occurs with certain plate and objective combinations, but as this is supposed to be a general protocol (irrespective of specific HCS microscope type), we felt it best to advise not using the outer wells of the plate.

Figure 1 doesn't show that a Matrigel overlay is added on top of spheroids - I would change that to add.

Figure 1 has been modified to better represent this.

## Reviewer #2:

### Manuscript Summary:

This manuscript describes a protocol for large-scale generation of tumor spheroids for high-content screening (HCS) applications showing some experimental results with three selected solid tumor cell lines: NCI-H358 (NSCLC), HepG2 (hepatocellular carcinoma) and HT-29 (colorectal adenocarcinoma).

Although the approach is not entirely new and there is a significant body of literature on HCS analysis of 3D models, the authors provide useful tips focusing on some critical aspects related to the formation of multispheroids (several hundred) per well instead of a single spheroid, to the plate type, the extracellular matrix and imaging parameters. Furthermore, they highlight the importance of combining low-resolution volumetric analysis of the whole spheroid with high-resolution phenotypic analysis of the individual cells within the spheroid.

### Major Concerns:

1. After cell seeding, the medium is replaced every second day with fresh phenol red-free complete medium: is it always necessary, or the frequency of medium change is somehow cell line dependent? In principle, changing the medium can interfere with the growth of spheroids and complicate the screening of compounds, since this would imply that the compound should also be administered at the same dose along with the fresh culture medium every second day. The Authors should provide some example of cell treatment experiments using this protocol.

It is not always necessary to change the medium every second day; this is indeed cell line-dependent. Regular medium exchange is advisable if the spheroids are to be maintained in an active growth phase. We agree that when incubating the spheroids with compounds, this regular changing of medium would add complexity to the assay. Previous work in our own laboratory in which we incubate spheroids with nanoparticles, has shown that these can be left on cells for up to 72 h without further medium exchange during this time (see references 16 and 17 in the revised manuscript).

2. How many days can the spheroids be cultured, and possibly treated with compounds (siRNA, sgRNA, etc), using this procedure? Is it possible to adapt this protocol also for live-cell kinetic analyses (e.g. using cell lines expressing fluorescent proteins)?

In the protocol presented here, with these particular cell lines, we only culture the spheroids for up to 7 days in order to generate the size ranges as shown. However, in previous studies we have used this protocol to grow spheroids for up to 15 days (reference 16), which includes an incubation with nanoparticles for the final 72 h, as well as incubations with siRNAs for up to 7 days. Although we have only conducted a small number of live cell imaging studies with these spheroids, our preliminary data suggest that this protocol is indeed also suitable for this application. We have added a note to this point in the Discussion of the revised manuscript.

-

3. Why are only 60 inner wells of the 96 plate typically used, excluding the ones on the plate border? Do the spheroids grow less in the perimeter wells, or is there more evaporation, or the extracellular matrix (matrigel) is less homogeneous, or something else? It would be interesting to discuss this aspect in more detail to understand if it can be addressed.

We have added a note about this to the protocol. The reason that we advise only using the central 60 wells, is that with some plate types, the high NA objectives are unable to image the outer wells as they physically make contact with the 'skirt' of the plate. This then precludes imaging of that entire well without potentially causing damage to the objective lens. This problem only occurs with certain plate and objective combinations, but as this is supposed to be a general protocol (irrespective of specific HCS microscope type), we felt it best to advise not using the outer wells of the plate.

4. The Authors state that, depending on the cell line or the desired spheroid properties, spheroids with dimensions below 75  $\mu\text{m}^3$  or above 900  $\mu\text{m}^3$  are typically discarded. The reason why small spheroids are discarded is easily understood, however there are some concerns about the upper limit of the size of individual spheroids. On the one hand, it is obviously necessary to prevent the spheroids from fusing with each others (as shown in figure 6), but on the other hand, spheroids that are not large enough hardly acquire the key characteristics of this type of model: heterogeneity (e.g., less proliferating/necrotic core and proliferating outer layer), gradient of oxygen, nutrients, etc. From the data presented in figure 4A it appears that the acquired spheroids contain on average 10-20 cells, thus they substantially are microcolonies: are spheroids of this size useful as a model? Would it be possible to seed fewer cells and cultivate them for longer times to generate larger spheroids without them fusing with each other? What difficulties would this change imply?

Yes, as indicated in our response to point 2, above, it is possible to grow larger spheroids when the cultures are maintained for longer periods of time (see also reference 16). This does require using fewer cells at the time of seeding (see references 16 and 17, which provide specific examples of this). The spheroids that we describe in this work are deliberately cultured for relatively short periods of time (and as such do not have a necrotic core), as we find that they suit the biological applications that we are typically evaluating. One major strength of our approach is that the method naturally generates a wide range of spheroid sizes in each well. We therefore use the power of HCS to select spheroids that have sizes or characteristics that fit our experiment. The examples given here are only examples, and we would refer the reviewer to

reference 17, where we show data for different size classes of spheroids, but all cultured in the same well. The researcher is free to select and analyse the size of spheroids that are relevant to their particular biological application. As can be seen in Figure 4, while there are indeed spheroids that typically contain ca. 20 cells, there are also spheroids with many more cells. Culturing the cells for longer naturally increases the overall size of the spheroids. These decisions need to be determined by the researcher.

Minor Concerns:

1. The volume of PBS used for washes is not specified in fix-permeabilization and immunostaining protocols;

These details have been added in the revised manuscript.

2. It is mentioned that the immunofluorescence staining of spheroids is adapted from Nürnberg et al, Front. Mol. Biosci 2020: if the protocol has been adapted from the one previously described, the Authors should specify if and in what the two protocols differ;

The key differences from the previously published paper are now mentioned in the revised manuscript (protocol 3).

3. "Permeabilization buffer" is a more appropriate term than "penetration buffer".

This change has been made in the revised manuscript.